Fast Parametric Curve Matching (FPCM) Filters for Deep Learning-Based Automatic Spike Detection

Anton S. Belokopytov(✉), Daria F. Kleeva, and Alex E. Ossadtchi

Higher School of Economics (National Research University), Moscow, Russia
asbelokopytov@edu.hse.ru

Abstract. Electroencephalography (EEG) is a valuable tool for the clinical localization of interictal spike sources. Typically, clinicians need to manually analyze and annotate all the data, a process that is time-consuming and prone to a high rate of false negatives. Recent advancements in mathematical algorithms and deep learning offer the possibility to automate this process. This work focuses on developing an algorithm using Fast Parametric Curve Matching (FPCM) filters to assist clinicians in classifying EEG data and detecting interictal spikes. The proposed method was trained on each FPCM coefficient, achieving an average ROC AUC of 0.967 ± 0.015, PR AUC of 0.9224 ± 0.021, and accuracy of 0.935 ± 0.012. These results suggest that while the method has potential, further development and optimization of the model architecture are necessary to fully realize its capabilities.

Keywords: Electroencephalography (EEG) · Epilepsy · Interictal spikes · Spike detection · Deep learning

1 Introduction

Electroencephalography (EEG) is the gold standard for diagnosing epilepsy [1, 2]. When a person experiences an event resembling a seizure, either through description or video evidence, especially if it occurs during sleep, EEG monitoring is crucial. The patient undergoes a video EEG monitoring session, including overnight sleep. If spikes are detected in specific regions, it suggests epileptiform activity. This finding prompts further investigation with magnetic resonance imaging (MRI) using epilepsy protocols to identify structural abnormalities like hippocampal sclerosis or tumours for instance [3, 4].

Typically, a recording of sufficient duration is enough for diagnosis. However, an automated detection system that processes data immediately would significantly reduce the workload for clinicians, allowing them to focus on reviewing marked spikes.

In more complex cases, patients might undergo multi-day video EEG monitoring to identify the cause of seizures, which may not be evident in structural MRI findings. Federal centers, which also conduct research, might register spikes over several days to

B. Kryzhanovsky et al. (Eds.): NI 2024, *Advances in Neural Computation, Machine Learning, and Cognitive Research VIII*, pp. 317–326, 2024.
https://doi.org/10.1007/978-3-031-73691-9_29

analyze various factors like the effect of medication withdrawal on epileptiform activity or changes in spike morphology.

The variability of interictal spikes presents a significant challenge for routine automatic detection. Interictal spikes can vary greatly in their morphology, amplitude, and frequency, making it difficult for standard detection algorithms to perform reliably across different patients and recordings.

To address this issue, it is suggested to personalize autodetection systems by incorporating additional training on annotated data specific to the patient. For instance, if a patient requires two or more routine day recordings, it could be beneficial to annotate only the first day's recording. Using this annotated data, a deep learning model can be trained and then its performance can be validated on subsequent days' recordings. This approach aims to leverage the personalized nature of the data, potentially improving detection accuracy and reliability. Model training has to be personalized so training data is limited by the data neurologist collected. In this paper, we attempt to solve exactly this task.

This problem has been explored by various research groups, leading to the development of different architectures to address it. Several conventional machine learning methods have been proposed for the automatic detection of interictal epileptiform discharges (IEDs) by extracting features from EEG signals in both time and frequency domains [5–7].

Most deep learning-based methods employ convolutional neural networks (CNNs) [8–10, 16], recurrent neural networks (RNNs) [11–13], and hybrid approaches [8, 11, 14] to detect IEDs in both scalp and intracranial EEG recordings; combined template-matching with CNN approaches [15].

Prasanth et al. [17] uses convolutional neural networks (CNNs) with a combination of raw EEG and frequency sub-bands. They arrange these sub-bands as a vector for one-dimensional CNN or a matrix for two-dimensional CNN to detect interictal epileptiform discharges (IEDs) effectively. Prasanth et al. (2020) tried to train the model using band-pass filters but in the current paper we would like to suggest the way of filtering which is very close to template. To enhance the training process, we apply the Fast Parametric Curve Matching (FPCM) method for feature extraction. The FPCM method, as detailed by Kleeva et al. [18], involves constrained parametric morphological model based on peak-wave shape parametrization to efficiently identify interictal spikes (picture 1). This technique enables the formation of spline coefficients that effectively capture the characteristic shapes of epileptiform spikes in EEG data. The specific spline coefficients c_1, c_2, c_3, c_4, c_5, and c_6 are defined as follows:

- c_1 and c_3 determine the left and right slopes of the peak, respectively;
- c_2 and c_4 are the intercepts for these linear segments;
- c_5 scales the parabolic curve that approximates the wave part of the interictal discharge, while c_6 acts as the wave's intercept.

These features are then used to train a deep learning model tailored to the patient's specific EEG patterns. The algorithm proposed in current paper is also inspired by the SincNet model developed by Hung et al. [19]. SincNet leverages parameterized sinc functions to learn the band-pass filters, effectively reducing the complexity and the learnable parameters within the convolutional layers of a neural network. This approach

demonstrates that using learned filters instead of traditional manually defined ones can lead to better feature extraction from raw audio signals with fewer parameters.

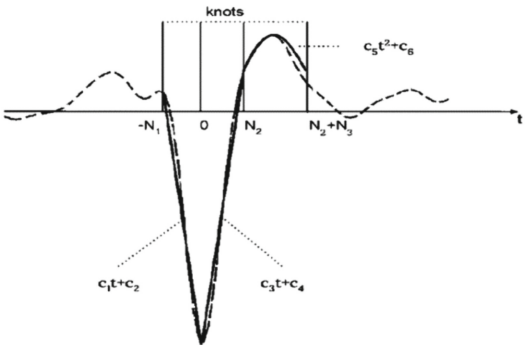

Fig. 1. The parametrization of the interictal spike shape (dotted line) with the spline (solid line).

Similar to the strategy used in SincNet, where trainable sinc functions form the core of the filtering process, the Fast Parametric Curve Matching (FPCM) approach also revolves around trainable parameters that define the length and shape of filters.

Due to the limited amount of data available at this stage, we present this work as a preliminary investigation rather than a result of thorough evaluation. We acknowledge that further validation with larger datasets is necessary to fully establish the reliability and robustness of the algorithm.

2 Materials and Methods

This study was conducted with approval from the Human Research Ethics Committee of The Research Center of Neurology, Moscow. EEG recordings and all related data collection were carried out at The Research Center of Neurology. All participants provided written informed consent in accordance with the Declaration of Helsinki.

2.1 EEG Data and Preprocessing

The EEG data used in this study were recorded during clinical examinations of epilepsy at the Scientific Center of Neurology from 2023 to 2024. The dataset consists of pairs of 24-h recording sessions with a stop division between them for each patient.

A bandpass filter with cutoff frequencies of 0.5 Hz and 35 Hz was applied to all data to reduce noise. Additionally, the data was downsampled from 256 Hz to 125 Hz.

To create the training, validation and testing dataset, the recordings were split into two classes: normal EEG (class 0) and interictal spikes (class 1). The data for class 0 were taken from healthy patients, while the data for class 1 were taken from epilepsy patients as annotated windows by neurologist. This approach ensured that the class 0 dataset was “clean” from the pathological abnormalities.

The process of preparation for class 0 and class 1 differs. For the creation of class 1, a neurologist annotated the centers of interictal spikes. After that, 1-s windows were created with 0.5-s steps to the right and left from the center.

To address the class imbalance and enhance the dataset, various data augmentation techniques were applied:

- **Jittering**: Each window was jittered by 50 samples to both sides to introduce variability and reduce overfitting.
- **Filtering**: The windows were filtered using different frequency bands to generate additional data and capture various signal characteristics.
- **Synthetic Data Generation**: Synthetic EEG epochs were generated using a lead field matrix to simulate realistic EEG signals and further augment the dataset.

Before augmentation, we utilized 106 annotated patterns from one patient: 94 patterns from day 1 for training/validation and 12 patterns from day 2 for testing. The augmentation process allowed us to increase the amount of training data to 9494 patterns.

Training epochs for class 0 were created by randomly selecting windows from healthy patients, in quantities twice as large as those for class 1, without augmentation and overlapping. Thus, the total count for class 0 of training dataset is 19,000 1-s patterns.

For the testing data of class 1, only jittering was applied as augmentation, considering that the auto analyzer could potentially observe patterns with different shifts from the center of the pattern. This increased the amount of testing data to 1200 samples for class 1. Jittering provides a probabilistic picture of pattern detection. Additionally, 5000 samples from day 2 recordings were taken as class 0 for testing, without overlapping.

To make the dataset more consistent, class 0 was aligned with class 1 [20], followed by Z-normalization of all windows. Alignment process can be described as following. Assume we have two data matrices X_1, X_2 representing EEG recordings from two different EEG windows, normalized to have zero mean. Our task is to make X_2 dataset share the same properties as X_1. Then covariance matrices C_1, C_2 for each dataset are calculated as following:

$$C_1 = \frac{1}{size(X_1[2])} * X_1 * X_1^T, \tag{1}$$

$$C_2 = \frac{1}{size(X_2[2])} * X_2 * X_2^T. \tag{2}$$

Then for each covariance matrix, the matrix square root is computed using eigenvalue decomposition:

$$sqrtC_2 = E_1 L_1^{\frac{1}{2}} E_1^T, \tag{3}$$

$$sqrtC_2 = E_2 L_2^{\frac{1}{2}} E_2^T, \tag{4}$$

where L is the diagonal matrix of eigenvalues and E is the matrix of eigenvectors. And the last step of alignment is following:

$$X_{2aligned} = sqrtC_1 * inv(\text{sqrt}C_2) * X_1 \tag{5}$$

It's valuable to note that the X_1 matrix was built as the concatenation of all interictal spikes from the training dataset. X_2 represents any 1-s epoch that we want to align to X_1, such as epochs from the second day's recording. This method helps us align the data to the interictal spikes.

After alignment all the data goes through the process of Z-standardization by the formula:

$$x_0 = \frac{x_i - \mu}{\sqrt{\sigma^2}}, \tag{6}$$

where x_i and x_0 represents the filtered data and the standardized output data accordingly. μ and σ^2 are the mean and variance calculated based on the training data and are used directly for the test data.

Thus, the training data have the picture like structure of batch_size × EEG_channels × time_series.

2.2 Model Architecture

The valuable part of model architecture is the use of FPCM coefficients which is implemented as a separate layer in keras python package (Fig. 2).

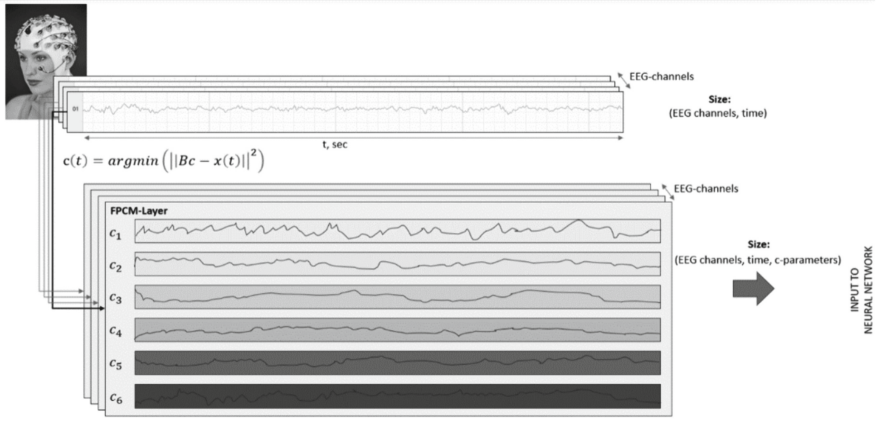

Fig. 2. Implementation of the FPCM layer

Kleeva et al. (2021) parameterized the shape of the interictal spike using the following equation:

$$s(t) = \begin{cases} c_1 t + c_2 if\ -N_1 \le t \le 0, \\ c_3 t + c_4 if\, 0 \le t \le N_2, \\ c_5 t^2 + c_6 if N_2 \le t \le N_2 + N_3 \end{cases}, \tag{7}$$

so that c_1 and c_3 are the peak's left and right slopes, c_2 and c_4 are the corresponding intercepts, c_5 scales the parabolic curve approximating the wave part of the interictal discharge and c_6 is wave's intercept.

After that, the authors tried to find a solution to the equation

$$c(t) = argmin\big(||Bc - x(t)||^2\big), \tag{8}$$

where $x(t) = [x(t - N_1), x(t - N_1 + 1), \ldots, x(t + N_2 + N_3)]^T$ is a single channel data segment, centered around the peak of the spike's sharp wave, $c(t) = [c_1(t), \ldots, c_6(t)]^T$ is the vector of resulting spline coefficients for data segment $x(t)$, and B is the morphological model matrix (Fig. 1).

Omitting details, the solution of Eq. 8 can be found as following:

$$c(t) = B^{\dagger}x(t). \tag{9}$$

All in all, the implemented layer extracts morphological coefficients for all EEG data points, creating a tensor with the size of batch_size × EEG_channels × time_series (1 s) × coefficient_channels (6 coefficients). After getting the coefficients, they are concatenated with the original EEG signal, so the tensor gains a 7th channel. Following this, all channels are flattened into a single sequence along the time axis. The resulting model structure is represented in Fig. 3.

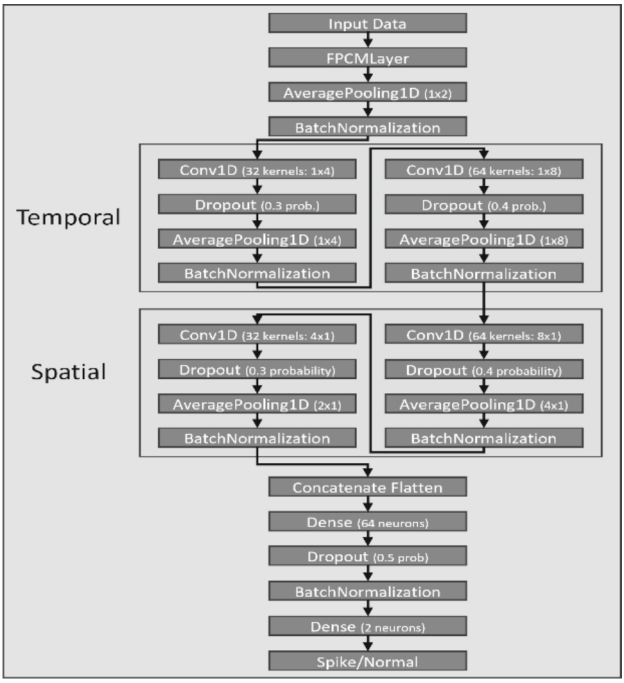

Fig. 3. Proposed model architecture**.** The model uses ReLU activation functions in all layers except the final layer, which uses a sigmoid activation function. The Adam optimizer was used with a learning rate set to 0.001. The binary cross-entropy loss function was used for training.

Such a structure is reminiscent of the approach described in the paper "Deep Learning for Interictal Epileptiform Spike Detection from Scalp EEG Frequency Sub-bands" by Thangavel Prasanth et al. [17]. In that work, they utilize CNN architectures to process and analyze EEG sub-bands, demonstrating the effectiveness of combining frequency-based features for improved spike detection performance. The input to their CNN is a combination of raw EEG and frequency sub-bands arranged either as a vector for one-dimensional (1D) CNN or a matrix for two-dimensional (2D) CNN. This approach aids in leveraging both the spatial and temporal information inherent in EEG signals, enhancing the detection accuracy of interictal epileptiform discharges (IEDs). Their results showed a 1D CNN-based IED detector with multiple sub-bands achieving a false positive rate per minute of 0.23 and a precision of 0.79 at 90% sensitivity, highlighting the potential of combining different EEG sub-bands for more accurate IED detection.

Since it's necessary to evaluate the efficiency of the FPCM layer, it's not needed to overcomplicate the model structure because it's enough to delete it for comparison with the baseline. For the FPCM layer trainable parameters are biases and the lengths of different morphological structure of matrix B, mentioned in Eqs. 8, 9.

2.3 Training and Evaluation Process

For the training process, we utilized a batch size of 32. The model was trained on a dataset corresponding to the first day for each patient, while the evaluation was conducted on the data from the second day.

The training and evaluation were performed using a 5-fold cross-validation method to ensure robust evaluation. The dataset was divided into five folds, with each fold used separately for training and validation. The model was built using a custom function that included the FPCM layer for morphological feature extraction. During training, the model was fitted with a batch size of 32 for three epochs for each fold.

The model's performance was assessed using several metrics, including accuracy, ROC AUC, and Precision-Recall AUC (PR AUC). A confusion matrix was employed to calculate the number of false positives and false negatives. For each evaluation metric, the mean and standard error of the mean (SEM) were computed, and a 95% confidence interval was calculated using the t-distribution.

Additionally, we calculated the false positive rate per minute and the false negative rate.

3 Results

All the results are presented in the Table 1.

The results indicate that training the model on each coefficient separately does not lead to a significant increase in performance when concatenated. This suggests that the chosen architecture may need adjustments to better estimate all coefficients.

Table 1. The model performance fitted on different FPCM coefficients.

Method and the measure	ROC AUC	PR AUC	Accuracy	FP/min	FN/min
No FPCM	0,969 ± 0,005	0,926 ± 0,013	0,944 ± 0,006	2,21 ± 0,33	1,167 ± 0,243
c_1 FPCM coefficient	0,935 ± 0,013	0,853 ± 0,02	0,901 ± 0,036	4,14 ± 2,85	1,86 ± 0,72
c_2 FPCM coefficient	0,937 ± 0,008	0,854 ± 0,021	0,926 ± 0,007	1,3 ± 0,75	3,18 ± 1,09
c_3 FPCM coefficient	0,921 ± 0,018	0,821 ± 0,055	0,913 ± 0,023	2,54 ± 1,43	3,02 ± 0,6
c_4 FPCM coefficient	0,938 ± 0,020	0,87 ± 0,025	0,932 ± 0,012	1,38 ± 1,25	2,72 ± 1,21
c_5 FPCM coefficient	0,903 ± 0,115	0,785 ± 0,282	0,842 ± 0,164	7,09 ± 10,46	2,43 ± 2,47
c_6 FPCM coefficient	0.938 ± 0.023	0.868 ± 0.039	0.935 ± 0.011	1,17 ± 0,21	2,77 ± 0,63
Concatenated coefficients	0,967 ± 0,015	0,9224 ± 0,021	0,935 ± 0,012	2,25 ± 1,76	1,66 ± 1,05

4 Conclusion

This study demonstrates that while the FPCM method provides a promising approach for feature extraction in EEG data, the current model architecture may require further refinement to maximize its effectiveness. Future work will focus on optimizing the architecture and exploring additional methods to enhance the performance of automatic spike detection algorithms.

Acknowledgement. This article is an output of a research project implemented as part of the Basic Research Program at the National Research University Higher School of Economics (HSE University).

References

1. Staba, R.J., Stead, M., Worrell, G.A.: Electrophysiological biomarkers of epilepsy. Neurotherapeutics **11**(2), 334–346 (2014). https://doi.org/10.1007/s13311-014-0259-0
2. Noachtar, S., Rémi, J.: The role of EEG in epilepsy: a critical review. Epilepsy Behav. **15**, 22–33 (2009). https://doi.org/10.1016/j.yebeh.2009.02.035
3. Duncan, J.S.: Brain imaging in epilepsy. Pract. Neurol. **19**(5), 438–443 (2019). https://doi.org/10.1136/practneurol-2018-002180
4. Middlebrooks, E.H., Ver Hoef, L., Szaflarski, J.P.: Neuroimaging in epilepsy. Curr. Neurol. Neurosci. Rep. **17**(4), 32 (2017). https://doi.org/10.1007/s11910-017-0746-x
5. Wilson, S.B., Emerson, R.: Spike detection: A review and comparison of algorithms. Clin. Neurophysiol. **113**(12), 1873–1881 (2002). https://doi.org/10.1016/S1388-2457(02)00297-3
6. da Silva Lourenço, C., Tjepkema-Cloostermans, M.C., van Putten, M.J.A.M.: Machine learning for detection of interictal epileptiform discharges. Clin. Neurophysiol. **132**(7), 1433–1443 (2021). https://doi.org/10.1016/j.clinph.2021.02.403
7. El-Samie, F.E.A., Alotaiby, T.N., Khalid, M.I., Alshebeili, S.A., Aldosari, S.A.: A review of EEG and MEG epileptic spike detection algorithms. IEEE Access **6**, 60673–60688 (2018). https://doi.org/10.1109/ACCESS.2018.2875487
8. Jing, J., et al.: Development of expert-level automated detection of epileptiform discharges during electroencephalogram interpretation. JAMA Neurol. **77**(1), 103–108 (2020). https://doi.org/10.1001/jamaneurol.2019.3485
9. Tjepkema-Cloostermans, M.C., de Carvalho, R.C.V., van Putten, M.J.A.M.: Deep learning for detection of focal epileptiform discharges from scalp EEG recordings. Clin. Neurophysiol. **129**(10), 2191–2196 (2018). https://doi.org/10.1016/j.clinph.2018.06.024
10. Fürbass, F., Kural, M.A., Gritsch, G., Hartmann, M., Kluge, T., Beniczky, S.: An artificial intelligence-based EEG algorithm for detection of epileptiform EEG discharges: Validation against the diagnostic gold standard. Clin. Neurophysiol. **131**(6), 1174–1179 (2020). https://doi.org/10.1016/j.clinph.2020.02.032
11. Fukumori, K., Nguyen, H.T.T., Yoshida, N., Tanaka, T.: Fully data-driven convolutional filters with deep learning models for epileptic spike detection. In: Proceedings IEEE International Conference on Acoustics, Speech and Signal Processing (ICASSP). (ICASSP), pp. 2772–2776. IEEE (2019). https://doi.org/10.1109/ICASSP.2019.8682196
12. Xu, Z., Wang, T., Cao, J., Bao, Z., Jiang, T., Gao, F.: BECT spike detection based on novel EEG sequence features and LSTM algorithms. IEEE Trans. Neural Syst. Rehabil. Eng. **29**, 1734–1743 (2021). https://doi.org/10.1109/TNSRE.2021.3107142

13. Geng, D., Alkhachroum, A., Bicchi, M.A.M., Jagid, J.R., Cajigas, I., Chen, Z.S.: Deep learning for robust detection of interictal epileptiform discharges. J. Neural Eng. **18**(5), 056015 (2021). https://doi.org/10.1088/1741-2552/abf28e
14. Wei, B., Zhao, X., Shi, L., Xu, L., Liu, T., Zhang, J.: A deep learning framework with multi-perspective fusion for interictal epileptiform discharges detection in scalp electroencephalogram. J. Neural Eng. **18**(4), 0460b3 (2021). https://doi.org/10.1088/1741-2552/ac0d60
15. Lourenço, C., Tjepkema-Cloostermans, M.C., Teixeira, L.F., van Putten, M.J.A.M.: Deep Learning for Interictal Epileptiform Discharge Detection from Scalp EEG Recordings. In: Henriques, J., Neves, N., de Carvalho, P. (eds.) MEDICON 2019. IP, vol. 76, pp. 1984–1997. Springer, Cham (2020). https://doi.org/10.1007/978-3-030-31635-8_237
16. Clarke, S., et al.: Computer-assisted EEG diagnostic review for idiopathic generalized epilepsy. Epilepsy Behav. **121**(Pt B), 106556 (2021). https://doi.org/10.1016/j.yebeh.2019.106556
17. Prasanth, T., et al.: Deep learning for interictal epileptiform spike detection from scalp EEG frequency sub-bands. In: Proceedings Annual International Conference of the IEEE Engineering in Medicine and Biology Society, pp. 3703–3706. IEEE (2020). https://doi.org/10.1109/EMBC44109.2020.9175644
18. Kleeva, D., Soghoyan, G., Komoltsev, I., Sinkin, M., Ossadtchi, A.: Fast parametric curve matching (FPCM) for automatic spike detection. J. Neural Eng. **19**(3) (2022). https://doi.org/10.1088/1741-2552/ac682a
19. Hung, C.-H., Wang, S.-S., Wang, C.-T., Fang, S.-H.: Using SincNet for learning pathological voice disorders. Sensors **22**(17), 6634 (2022). https://doi.org/10.3390/s22176634
20. Yair, O., Dietrich, F., Talmon, R., Kevrekidis, I.G.: Domain adaptation with optimal transport on the manifold of SPD matrices. arXiv preprint arXiv:1906.00616v4 (2020). https://doi.org/10.48550/arXiv.1906.00616